When dilution resolves a low sandwich-immunoassay signal: robust certificates and the limits of spike controls

Abstract

A low sandwich-immunoassay signal can mean little analyte, or so much analyte that capture and detection reagents are spread over different molecules (the high-dose hook effect). We ask what a second reading of a diluted aliquot certifies in a finite-reagent, independent-site equilibrium model when capacities, affinities, dilution factor, gain drift and native availability are known only to within intervals. The noise-free ambiguity is described exactly: the response is strictly unimodal, every sub-maximal signal has exactly two preimages (exchanged by an involution for symmetric sites), and the diluted-to-neat ratio is strictly increasing. We then prove robust two-reading certificates: for near-unit parameters, dilution in $[9, 11]$ and 5% gain drift, the diluted-minus-neat source contrast is nonpositive for accessible concentration at most 0.4 and at least 0.04 on $[20, 100]$; a general-box theorem gives analogous margins when capacities exceed dissociation constants a hundredfold, for unequal capacities, and up to 10^4 with an explicit $1/U$ law. Each continuum inequality reduces to eight positive Bernstein coefficients. We derive error budgets from precision profiles, a reduction of relative error to gain drift, conclusions without a binary promise and extensions to availability drift and incomplete equilibration, with a kinetic theorem giving a sufficient incubation time. Exact indistinguishability results show what a neat reading, accessible spikes and finite dilution panels cannot certify. For sequential assays, ideal washing gives a monotone saturating response, any fixed carry-over restores the high-dose tail, and a finite-range wash specification is given. The source inequalities, decisions, certificates and obstructions are verified in Lean 4; the structural and kinetic theorems have conventional proofs. These are conditional certificates, not clinical performance claims.

1 Introduction

1.1 The inference problem

In a two-site (sandwich) immunoassay an analyte is recognised by a capture reagent and by a labelled detection reagent, and the measured signal reports analyte that carries both [19, 34]. When capture and detection reagents meet the specimen simultaneously, the response is not monotone. At sufficiently high concentration the finite reagent supplies are distributed over different analyte molecules, doubly occupied complexes become rare, and the signal falls back towards the blank. This high-dose hook (or prozone) effect has been analysed experimentally and theoretically for decades [25, 23, 24, 28, 8], remains a recognised source of falsely low results in clinical chemistry [31, 33, 32, 12], and belongs to the wider family of bell-shaped three-body binding responses [5, 27].

The standard remedy is dilution: if a diluted aliquot reads *higher* than the neat specimen, the neat reading was on the descending limb [2, 15], and dilution linearity with an explicit hook check is part of ligand-binding assay validation [4, 14]. Upfront dilution has improved a ferritin workflow [35]; reaction-rate monitoring and real-time kinetics flag antigen excess or extend the usable range [11, 22, 30]; but dilution also degrades accuracy when the specimen matrix departs from the validated one [13], and in lateral-flow formats even the control line can depend on concentration [26]. The practical question is therefore not whether dilution can help. It is what, exactly, a neat/diluted

pair of raw readings certifies when nothing about the assay is known exactly: reagent capacities and affinities lie in calibration intervals, a nominal tenfold dilution is really a factor somewhere in $[9, 11]$, the instrument gain drifts between the two readings, readings carry error, and only a fraction of the native analyte may be recognisable by the antibody pair.

1.2 Contributions

We treat this as a problem of robust inference under a mass-balance source model with interval-valued calibration, in the spirit of partial identification [17]: a conclusion is admissible only if it holds for every state of the world compatible with the declared assumptions. The contributions are as follows.

1. *Exact structure of the ambiguity* (Section 3). For every parameter choice the equilibrium response $B(u)$ is strictly unimodal, its logarithmic slope decreases strictly from 1 to -1, every sub-maximal level has exactly two preimages, and the diluted-to-neat ratio $B(u/d)/B(u)$ increases strictly from $1/d$ to d. When the two sites have equal $C + K = D + J = S$ the two preimages are exchanged by $u \mapsto S^2/u$. Hence a neat reading is ambiguous for every assay in the model class, and the sign of the dilution contrast has a single crossover concentration.

2. *A robust two-reading certificate* (Section 4). We prove uniform source margins over full calibration boxes by retaining the reagent product shared by both readings and reducing a two-variable polynomial inequality to eight positive Bernstein coefficients. A general-box theorem covers arbitrary positive calibration intervals; worked instances include a near-unit box, a high-capacity regime with $C/K \approx 100$, unequal capture and detector capacities, and ranges up to 10^4 with an explicit $7371/(8000\,U)$ law.

3. *From margins to decisions* (Section 5). Additive-error budgets, one-sided exclusions that need no low-or-high promise, a sound outer enclosure of the compatible concentrations, a bridge from a precision profile to a deterministic error allowance with stated coverage, and an exact reduction of bounded relative error to gain drift.

4. *Exact limits* (Section 6). Three observational equivalences show what cannot be certified: a neat reading alone; native concentration from fully accessible spikes when native masking persists; and exclusion of an unbounded high tail by any finite dilution panel with nonzero error. The sufficient operating ceiling and the obstruction both scale as $1/\varepsilon$.

5. *Departures from the ideal protocol* (Section 7). Availability that changes on dilution is an effective change of dilution factor; a calibrated attenuation bound suffices for incompletely equilibrated readings; and for well-mixed mass-action kinetics started unbound we prove the attenuation bound $(1 - e^{-\lambda_C t})(1 - e^{-\lambda_D t})$ with explicit rates, which converts rate constants into a sufficient incubation time.

6. *Sequential assays* (Section 8). With ideal washing the response is strictly increasing and approaches a positive plateau at an explicit rate; with any carry-over fraction $\lambda > 0$ it decays like $CD/(\lambda u)$; and a wash specification $\lambda_{\max} U \le D_{\min}(\beta^{-1} - 1)$ preserves a fraction β of the ideal signal on a finite range.

1.3 Evidence levels and scope

Statements are tagged L when the displayed statement has been compiled in Lean 4 with mathlib [3, 18] under the strict regime described in Section 10 (Table 6 lists the declarations), and C when

the proof is the conventional one given here. Numerical illustrations are labelled as such and carry no claim. All worked numbers are replayed by a script distributed with the source.

We do not claim priority for dilution protocols, kinetic rescue, mass-action models of the hook effect, or partial identification; the closest modelling work [24, 8, 9, 5, 21] derives and fits response curves, whereas the present paper asks which decisions remain valid uniformly over calibration uncertainty and proves them. We do not establish a clinically superior protocol. The model is homogeneous, noncooperative and two-site; immobilised reagents, multivalency, cooperative binding [27], transport in lateral-flow strips [21, 26] and matrix effects are outside it, and the assumptions are part of every result.

2 Source, protocol and observation model

2.1 Finite-reagent equilibrium

Let $x \geq 0$ be the total native analyte concentration and $u = \rho x$ the concentration that is accessible to both antibodies, where $\rho \in (0, 1]$ is an availability fraction. The analyte has two distinct, independent binding sites. The effective capture and detector binding-site capacities are $C, D > 0$ and the site dissociation constants are $K, J > 0$; all concentrations refer to the final reaction volume. Writing $p, q \in (0, 1)$ for the occupied fractions of the two sites on accessible analyte, conservation of each reagent gives

$$C = up + \frac{Kp}{1-p}, \qquad D = uq + \frac{Jq}{1-q}, \qquad B(u) = upq. \tag{2.1}$$

The four analyte species $u(1-p)(1-q)$, $up(1-q)$, $u(1-p)q$, upq are nonnegative and sum to u; the free reagents are $C_f = Kp/(1-p)$ and $D_f = Jq/(1-q)$. The identities $C_f(1-p) = Kp$ and $D_f(1-q) = Jq$ are the four mass-action equilibria with the same site constant whether or not the other site is occupied; this is the independent-site assumption. Thus (2.1) is a mass-balance source and not a fitted hook-shaped curve. The signal-generating species is the doubly occupied complex $B(u)$. The capture equation is a quadratic for $w = up$, namely $(C-w)(u-w) = Kw$, whose physical root gives the numerically stable expression

$$p(u; C, K) = \frac{2C}{u + C + K + \sqrt{(u-C)^2 + 2K(u+C) + K^2}}, \tag{2.2}$$

used for illustrations only. The proofs use (2.1) directly.

Lemma 2.1 (Physical root and envelopes; L)**.** *For $u \geq 0$ and $C, K > 0$ the capture equation in (2.1) has exactly one root $p \in (0, 1)$, and*

$$\frac{C}{u+K+C} \leq p \leq \frac{C}{u+K}, \qquad up \leq C. \tag{2.3}$$

The same holds for the detector site, and therefore

$$\frac{CDu}{(u+K+C)(u+J+D)} \leq B(u) \leq \frac{CDu}{(u+K)(u+J)}, \qquad B(u) \leq u, \qquad uB(u) \leq CD. \tag{2.4}$$

Proof. The polynomial $(C-up)(1-p) - Kp$ is positive at $p = 0$ and negative at $p = 1$, so a root exists; the right side of the capture equation is strictly increasing in p, so it is unique. Mass balance gives $C \geq (u+K)p$, and $K/(1-p) = K + C_f \leq K + C$ gives $C \leq (u+K+C)p$. Multiplying the two sites' bounds gives the envelopes, $p, q < 1$ gives $B \leq u$, and $up \leq C$, $uq \leq D$ give $uB \leq CD$. □

The envelopes already exhibit both tails. For small u the response is linear, $B(u) \sim \alpha u$ with $\alpha = CD/((C+K)(D+J))$; for large u,

$$B(u) = \frac{CD}{u} - \frac{CD(K+J)}{u^2} + O(u^{-3}), \tag{2.5}$$

because each limited reagent population is spread over many analyte molecules. A monotone Hill curve has no such second tail; conversely, (2.1) is one architecture and not every sandwich assay.

2.2 Protocol, calibration box and observations

Two matched reactions are prepared. The specimen is diluted by a factor d *before* fresh reagents are added, so that both reactions have the same C, D, K, J in the same final volume. Diluting an already assembled reaction changes C and D as well and is a different experiment. The blank-corrected raw readings and their contrast are

$$Y_1 = gB(u) + e_1, \qquad Y_d = grB(u/d) + e_d, \qquad Z = Y_d - Y_1, \tag{2.6}$$

with common gain $g \geq g_{\min} > 0$, relative gain r between the readings, and additive errors with $|e_1|, |e_d| \leq \varepsilon$. The error allowance is one simultaneous deterministic bound that includes every admitted additive contribution once; no distribution or independence is assumed (Section 5.3 connects it to a precision profile). The running example is the *near-unit box*

$$C, D, K, J \in [\tfrac{9}{10}, \tfrac{11}{10}], \qquad d \in [9, 11], \qquad r \in [\tfrac{19}{20}, \tfrac{21}{20}], \qquad \rho \in [\tfrac{4}{5}, 1]. \tag{2.7}$$

The source contrast is $\Delta(u) = rB(u/d) - B(u)$, so that $Z = g\Delta(u) + e_d - e_1$.

Units. Concentrations are expressed relative to a chosen scale c_0 ($x = x_{\text{phys}}/c_0$, and likewise for C, D, K, J); raw signals use a separate scale. A change of units cannot force the four ratios among C, D, K, J to be near one, so (2.7) is a genuine restriction. Section 4.2 removes it.

Availability. The factor ρ is a two-population reduction: fully recognised analyte at concentration u, plus analyte invisible to the pair. Partially masked analyte that still consumes one reagent acts as a competitor and needs a larger model.

3 The exact structure of the ambiguity

Before adding uncertainty we describe the noise-free source completely. Let $E_C(u) = -u\,p'(u)/p(u)$ be the elasticity of the capture occupancy, E_D the detector analogue, and $L_B = \mathrm{d}\log B/\mathrm{d}\log u$.

Theorem 3.1 (Unimodality, two preimages, monotone ratio; C). *Fix $C, D, K, J > 0$ and $d > 1$.*

(i) $E_C = 1 - Kp/(C(1-p)^2 + Kp^2)$; it increases strictly from 0 to 1 on $(0, \infty)$, and $L_B = 1 - E_C - E_D$ decreases strictly from 1 to -1.

(ii) B is strictly increasing on $(0, u^*]$ and strictly decreasing on $[u^*, \infty)$ for a unique u^*, with $B(0^+) = B(\infty) = 0$. Every level $s \in (0, B(u^*))$ has exactly two preimages $u_-(s) < u^* < u_+(s)$.

(iii) The ratio $R(u) = B(u/d)/B(u)$ is strictly increasing, with $R(0^+) = 1/d$ and $R(\infty) = d$.

(iv) For $1/d < r < d$ there is a unique crossover $u^\dagger$ with $R(u^\dagger) = 1/r$, and $\Delta(u) < 0$ for $0 < u < u^\dagger$ while $\Delta(u) > 0$ for $u > u^\dagger$.

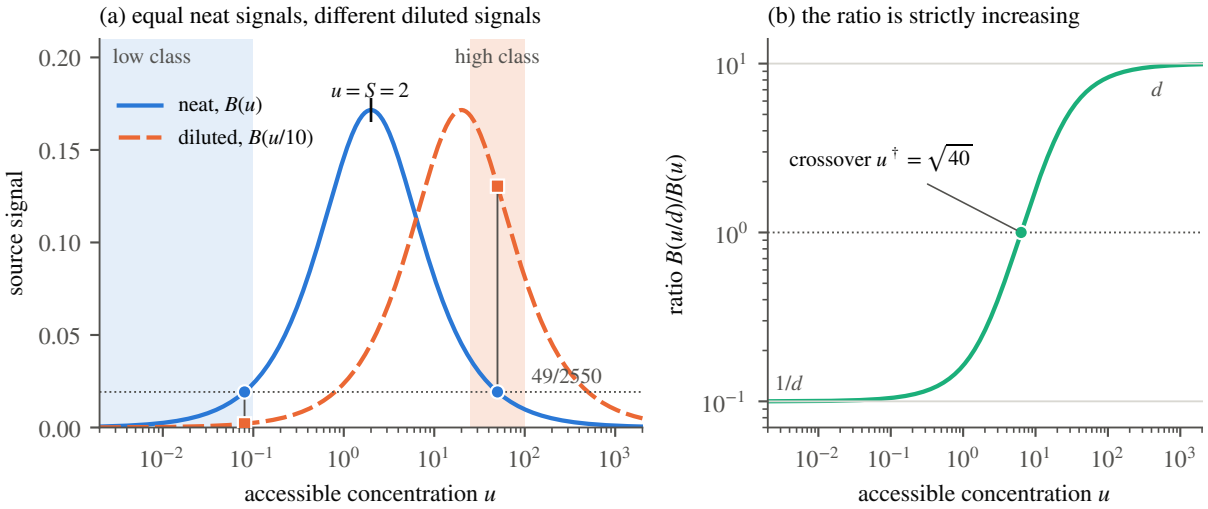

Figure 1: Synthetic source responses for $C = D = K = J = 1$ and $d = 10$. (a) The marked states (3.2) have equal neat signals and different diluted signals; the neat curve is symmetric under $u \mapsto 4/u$. (b) The ratio $B(u/d)/B(u)$ increases strictly from $1/d$ to d; with $r = 1$ the contrast changes sign at $u^\dagger = \sqrt{40}$. Floating-point illustration; the statements are proved in Section 3.

Proof. Differentiating $C = up + Kp/(1-p)$ gives $p' = -p/(u + K/(1-p)^2) < 0$, so $E_C = u(1-p)^2/(u(1-p)^2 + K)$. Substituting $u(1-p)^2 = (1-p)(C(1-p) - Kp)/p$ from the balance, and writing $Q = C(1-p)^2 + Kp^2$, the numerator becomes $Q - Kp$ and the denominator Q, hence $E_C = 1 - Kp/Q$. A direct computation gives

$$\frac{\mathrm{d}E_C}{\mathrm{d}p} = -\frac{K\{C - (C+K)p^2\}}{Q^2}.$$

At $u = 0$ the balance gives $p = C/(C+K)$, and p decreases in u, so $p^2 \le (C/(C+K))^2 < C/(C+K)$ and the derivative is negative. Since p decreases in u, E_C increases in u. At $p = C/(C+K)$ one finds $Q = CK/(C+K)$ and $Kp/Q = 1$, so $E_C(0^+) = 0$; as $u \to \infty$, $p \to 0$, $Q \to C$ and $E_C \to 1$. This proves (i), because $\log B = \log u + \log p + \log q$. For (ii), L_B is continuous and strictly decreasing from 1 to -1, so it has a unique zero u^*; the limits of B follow from (2.4). For (iii), $\mathrm{d}\log R/\mathrm{d}\log u = L_B(u/d) - L_B(u) > 0$ since $u/d < u$. The limits follow from $B(u) \sim \alpha u$ and $uB(u) \to CD$, both consequences of (2.4). Finally $\Delta = B(u)\,(rR(u) - 1)$ with $B > 0$ gives (iv). □

Proposition 3.2 (Hook involution; L for the first two sentences)**.** *Let $S = C + K$. If p is the capture occupancy at $u > 0$, then the capture occupancy at S^2/u is up/S. Consequently, if $C + K = D + J = S$, then*

$$B(S^2/u) = B(u) \qquad \text{for all } u > 0, \tag{3.1}$$

the maximum is at $u^* = S$, the two preimages in Theorem 3.1(ii) are $u_\pm$ with $u_- u_+ = S^2$, and for $r = 1$ the crossover is $u^\dagger = S\sqrt{d}$.

Proof. Put $u' = S^2/u$ and $p' = up/S$. Then $u'p' = Sp$ and

$$(C - u'p')(1 - p') - Kp' = \frac{1}{S}\{(C - Sp)(S - up) - Kup\} = (C - up)(1 - p) - Kp = 0,$$

using $S = C + K$ in the expansion. Moreover $0 < p' = up/S \le C/S < 1$ by (2.3), so p' is the physical root by Lemma 2.1. With both sites, $B(u') = u'\,(up/S)(uq/S) = upq$. Symmetry of a strictly unimodal function about $\log u = \log S$ puts the maximum at S and pairs the preimages. For $r = 1$, $\Delta(u) = 0$ means $B(u/d) = B(u)$ with $u/d \neq u$, so $u/d = S^2/u$. □

For unit parameters $S = 2$, the peak value is $B(2) = 3 - 2\sqrt{2}$, and the rational pair

$$(u, p, q) = \Big(\frac{200}{2499}, \frac{49}{100}, \frac{49}{100}\Big), \qquad \Big(\frac{2499}{50}, \frac{1}{51}, \frac{1}{51}\Big), \qquad \frac{200}{2499} \cdot \frac{2499}{50} = 4, \tag{3.2}$$

satisfies (2.1) exactly with the common signal $B = 49/2550$ (Figure 1a). Their tenfold-diluted signals are approximately 0.001993 and 0.130414. Theorem 3.1 shows that such a collision is not a feature of special parameters: *every* neat signal below the peak is produced by exactly two accessible concentrations, one on each limb, and the diluted-to-neat ratio separates them because it is injective. The rest of the paper asks how much of this ideal separation survives interval-valued calibration, gain drift, error and masking.

4 A robust two-reading certificate

4.1 Main theorem for the near-unit box

Theorem 4.1 (Source separation and noisy decision; L)**.** *Assume* (2.1), (2.6) *and the box* (2.7). *Then*

$$u \in [0, \tfrac{2}{5}] \implies \Delta(u) \le 0, \qquad u \in [20, 100] \implies \Delta(u) \ge \tfrac{1}{25}. \tag{4.1}$$

Consequently, for the native classes $x \in [0, \frac{2}{5}]$ (low) and $x \in [25, 100]$ (high),

$$Z \le 2\varepsilon \quad \textit{on the low class}, \qquad Z \ge g_{\min}/25 - 2\varepsilon \quad \textit{on the high class}, \tag{4.2}$$

and the rule "high if and only if $Z > 2\varepsilon$" separates the two classes whenever $4\varepsilon < g_{\min}/25$.

The source class is nonempty for every $x \ge 0$ (take unit parameters, unit gains, $d = 10$ and the physical roots; this is also compiled). The binary conclusion requires membership in one of the two declared classes; it says nothing about the guard band between them or about $x > 100$. Sections 5.2 and 6 treat both.

Proof. Low sign. For $0 \le u \le \frac{2}{5}$, Lemma 2.1 with $K + C, J + D \le a := \frac{11}{5}$ and $CD \ge \frac{81}{100}$ gives

$$B(u) \ge \frac{(81/100)\,u}{(u + 11/5)^2} \ge \frac{81}{676}\,u, \qquad rB(u/d) \le \frac{21}{20} \cdot \frac{u}{9} = \frac{7}{60}\,u,$$

and $\frac{7}{60} < \frac{81}{676}$. This includes $u = 0$.

Retaining the shared reagent product. Let $r_0 = \frac{19}{20}$. For $u > 0$, Lemma 2.1 applied at u/d and at u gives $B(u/d) \ge CD\,du/(u + ad)^2$ and $B(u) \le CD/u$ with the *same* factor CD, so

$$\Delta(u) \ge CD\Big\{\frac{r_0 du}{(u + ad)^2} - \frac{1}{u}\Big\}. \tag{4.3}$$

For a target margin $m > 0$ define

$$P_m(u, d) = 81\,r_0 du^2 - (81 + 100mu)(u + ad)^2. \tag{4.4}$$

Table 1: Exact Bernstein coefficients in (4.6) for the 0.04 source margin.

d	b_0	b_1	b_2	b_3
9	549739/25	6249899/25	23318059/25	554219/25
11	601099/25	25425377/75	34047819/25	26119179/25

If $P_m(u,d) \geq 0$, dividing by $u(u+ad)^2$ shows that the braces in (4.3) are at least $100m/81 \geq 0$, and $CD \geq 81/100$ then gives $\Delta \geq m$. No separate maximisation of the neat reagent product is used; doing so loses a factor of more than thirty in the margin (Remark 4.6).

Two dilution endpoints suffice. P_m is a concave quadratic in d, and for $9 \leq d \leq 11$ direct expansion gives

$$P_m(u,d) = \tfrac{11-d}{2} P_m(u,9) + \tfrac{d-9}{2} P_m(u,11) + \tfrac{121}{25}(81+100mu)(d-9)(11-d), \tag{4.5}$$

whose last term is nonnegative.

Eight coefficients. At either endpoint P_m is a cubic in u. With $u = 20+80t$, $0 \leq t \leq 1$, and $m = \frac{1}{25}$,

$$P_m(u,d) = b_0(1-t)^3 + 3b_1 t(1-t)^2 + 3b_2 t^2(1-t) + b_3 t^3 \tag{4.6}$$

identically in t, with the coefficients of Table 1. All are positive and every Bernstein basis function is nonnegative on $[0,1]$ [7, 10], so $P_m \geq 0$ on the whole rectangle $[20,100] \times [9,11]$. These are polynomial identities over the reals, not sampled corner tests.

Native classes and noise. For $\rho \in [\frac{4}{5}, 1]$, $x \leq \frac{2}{5}$ implies $u \leq \frac{2}{5}$ and $x \in [25,100]$ implies $u \in [20,100]$. Finally $Z = g\Delta + e_d - e_1$ with $|e_d - e_1| \leq 2\varepsilon$; $g > 0$ preserves the low sign and $g \geq g_{\min}$ the high bound. □

4.2 General calibration boxes

Nothing in the argument depends on the parameters being near one.

Theorem 4.2 (General-box certificate; L)**.** *Let $C, D, K, J > 0$ satisfy $K + C \leq A$, $J + D \leq H$ and $CD \geq c > 0$, let $u > 0$, $d > 0$, $r \geq r_0 \geq 0$ and $m \geq 0$, and put*

$$Q_m(u,d) = c\, r_0\, d\, u^2 - (c + mu)(u + Ad)(u + Hd). \tag{4.7}$$

(i) If $Q_m(u,d) \geq 0$ then $\Delta(u) = rB(u/d) - B(u) \geq m$.

(ii) For $d_- \leq d \leq d_+$, $(d_+ - d_-)\, Q_m(u,d) = (d_+ - d)\, Q_m(u,d_-) + (d - d_-)\, Q_m(u,d_+) + (d_+ - d_-)AH(c+mu)(d-d_-)(d_+-d)$; hence nonnegativity at the two dilution endpoints implies nonnegativity on $[d_-, d_+]$.

(iii) If $0 \leq u \leq u_L$, $d \geq d_{\min} > 0$, $0 \leq r \leq r_{\max}$ and

$$r_{\max}\,(u_L + A)(u_L + H) \leq c\, d_{\min}, \tag{4.8}$$

then $\Delta(u) \leq 0$.

Proof. (i) is the argument leading to (4.3) with $(u+Ad)(u+Hd)$ in place of $(u+ad)^2$: $Q_m \geq 0$ is equivalent to $c\{r_0 du/((u+Ad)(u+Hd)) - 1/u\} \geq m$, and $CD \geq c$. (ii) is an identity for a quadratic in d with leading coefficient $-AH(c+mu) \leq 0$. For (iii), $B(u) \geq cu/((u_L+A)(u_L+H))$ by (2.4) and $rB(u/d) \leq r_{\max} u/d_{\min}$ by $B(v) \leq v$. □

Table 2: Certified alternatives for the near-unit box (2.7). The error condition is for equal per-reading allowances and $g_{\min} = 1$; it is an absolute normalised signal allowance, not a coefficient of variation.

Accessible high range	Native high range	Source margin m	Error condition
$[20, 100]$	$[25, 100]$	0.04	$\varepsilon < 0.01$
$[12, 100]$	$[15, 100]$	0.01	$\varepsilon < 0.0025$
$[20, 1000]$	$[25, 1000]$	0.005	$\varepsilon < 0.00125$
$[20, 10000]$	$[25, 10000]$	0.0005	$\varepsilon < 0.000125$

For a box of calibration intervals one takes $A = K_{\max} + C_{\max}$, $H = J_{\max} + D_{\max}$, $c = C_{\min} D_{\min}$ and $r_0 = r_{\min}$. On a concentration interval $[L, U]$ the endpoint cubics $Q(u) = Q_m(u, d_\pm)$ have Bernstein coefficients

$$b_0 = Q(L), \quad b_1 = Q(L) + \tfrac{U-L}{3} Q'(L), \quad b_2 = Q(U) - \tfrac{U-L}{3} Q'(U), \quad b_3 = Q(U), \tag{4.9}$$

so a complete design check is the evaluation of eight rational numbers. A negative coefficient means that this sufficient certificate failed, not that the observations overlap; a narrower calibration box, a smaller margin or a subdivision of $[L, U]$ can then be tried. Theorem 4.1 is the instance $A = H = \frac{11}{5}$, $c = \frac{81}{100}$, for which $P_m = 100\, Q_m$.

Operating alternatives for the near-unit box. Table 2 lists four compiled certificates. Each row is a separate guarantee: the best threshold, range and margin of different rows cannot be combined. The low class is $[0, \frac{2}{5}]$ throughout.

Proposition 4.3 (Uniform range law; L)**.** *For the near-unit box, $u \geq 20$, $d \in [9, 11]$ and $r \geq \frac{19}{20}$,*

$$u\,\Delta(u) \geq \frac{7371}{8000}, \qquad \textit{so} \qquad \Delta(u) \geq \frac{7371}{8000\,U} \quad \textit{on } 20 \leq u \leq U. \tag{4.10}$$

Proof. By (4.3), $u\Delta \geq CD\{r_0\, d/(1 + 11d/(5u))^2 - 1\}$. For $u \geq 20$ the denominator is at most $(1 + 11d/100)^2$, and $4d - 9(1 + 11d/100)^2$ is a concave quadratic with values $\frac{3591}{10000}$ and $\frac{431}{10000}$ at $d = 9, 11$; hence $d/(1 + 11d/(5u))^2 \geq \frac{9}{4}$ and $u\Delta \geq \frac{81}{100}(\frac{19}{20} \cdot \frac{9}{4} - 1) = \frac{7371}{8000}$. □

Figure 2 compares the finite-range certificates with (4.10). Neither is an optimal frontier.

4.3 Capacities a hundred times the dissociation constants

Immunoassay reagents are often used at capacities far above their dissociation constants. The following synthetic design regimes show that the certificate is not confined to comparable scales. They are not measured parameters of any commercial assay.

Example 4.4 (High capacity; L)**.** Take $c_0 = 1$ nM and

$$C, D \in [9, 11] \text{ nM}, \qquad K, J \in [0.09, 0.11] \text{ nM},$$

with $d \in [9, 11]$, $r \in [\frac{19}{20}, \frac{21}{20}]$, $\rho \in [\frac{4}{5}, 1]$. The capacity-to-affinity ratio lies between about 82 and 122. Here $A = H = \frac{1111}{100}$ and $c = 81$. Condition (4.8) holds with $u_L = 15$ since $\frac{21}{20}(26.11)^2 \approx 715.8 \leq 729$, and the eight Bernstein coefficients of $Q_{2/5}$ on $[100, 1000]$ are positive (Appendix A). Therefore

$$x \leq 15 \text{ nM} \implies \Delta \leq 0, \qquad 125 \text{ nM} \leq x \leq 1000 \text{ nM} \implies \Delta \geq \tfrac{2}{5}, \tag{4.11}$$

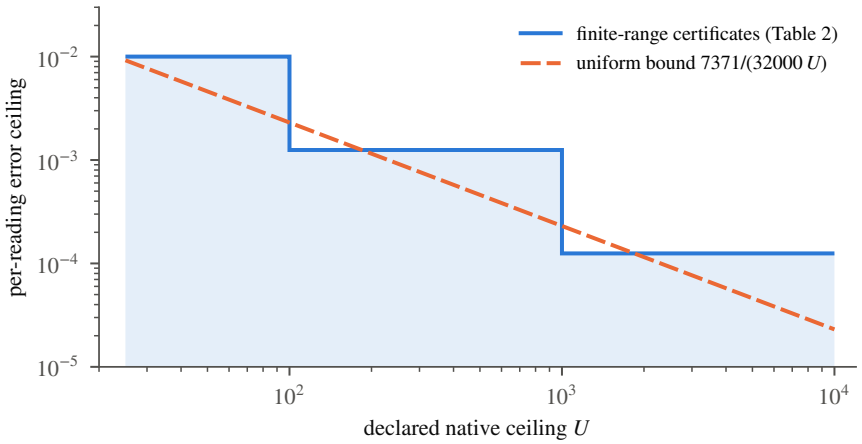

Figure 2: Sufficient per-reading error ceilings for the native high range $[25, U]$, $\rho \in [0.8, 1]$ and $g_{\min} = 1$. Steps: Table 2. Dashed: the uniform law (4.10), i.e. $\varepsilon < 7371/(32000\,U)$. Strictly smaller errors are certified.

Table 3: Example 4.4 at the central parameters $C = D = 10$, $K = J = 0.1$ nM, $\rho = 0.8$, $d = 10$, unit gains. Floating-point illustration; the proof is the coefficient table in Appendix A.

Native x (nM)	Accessible u (nM)	Neat $B(u)$	Diluted $B(u/10)$	Contrast
1	0.8	0.782904	0.078411	−0.704493
125	100	0.997782	8.187989	7.190207
500	400	0.249872	2.483435	2.233563
1000	800	0.124968	1.246437	1.121469

and with $g_{\min} = 1$ the decision survives any equal per-reading error $\varepsilon < 0.1$ in the normalised signal scale (one signal unit is the reading of 1 nM of doubly bound analyte at unit gain). A second certificate for the same box gives margin $\frac{3}{20}$ on accessible $[60, 1000]$, that is, native high class $[75, 1000]$ nM for $\varepsilon < 0.0375$. Table 3 gives central illustrations. The high class deliberately exceeds the reagent capacity: reagent excess over a normal measuring range is not reagent excess over every out-of-range specimen.

Example 4.5 (Unequal capacities; L)**.** Let $C \in [9, 11]$, $D \in [18, 22]$, $K \in [0.09, 0.11]$, $J \in [0.18, 0.22]$ nM, so that $A = \frac{1111}{100}$, $H = \frac{1111}{50}$, $c = 162$. Then (4.8) holds with $u_L = 20$ ($\frac{21}{20} \cdot 31.11 \cdot 42.22 \approx 1379 \le 1458$) and $Q_{4/5}$ has positive Bernstein coefficients on $[200, 1000]$: native $x \le 20$ nM gives $\Delta \le 0$, native $x \in [250, 1000]$ nM gives $\Delta \ge \frac{4}{5}$, and $\varepsilon < 0.2$ suffices at $g_{\min} = 1$. The classes and signal scales differ from those of Example 4.4, so the margins 0.8, 0.4 and 0.04 are not a ranking of designs.

Remark 4.6 (Tightness and the necessary guard band; numerical)**.** The admissible state $u = 100$, $d = 9$, $C = D = \frac{9}{10}$, $K = J = \frac{11}{10}$, $r = \frac{19}{20}$ has $\Delta \approx 0.0486095$, and a multistart search finds no smaller value on the high class, so the certified 0.04 is about 82% of the best possible uniform margin. The corresponding figures for Examples 4.4 and 4.5 are 0.4 against about 0.610 and 0.8 against about 1.218. An earlier version of the argument, which bounded the two readings independently,

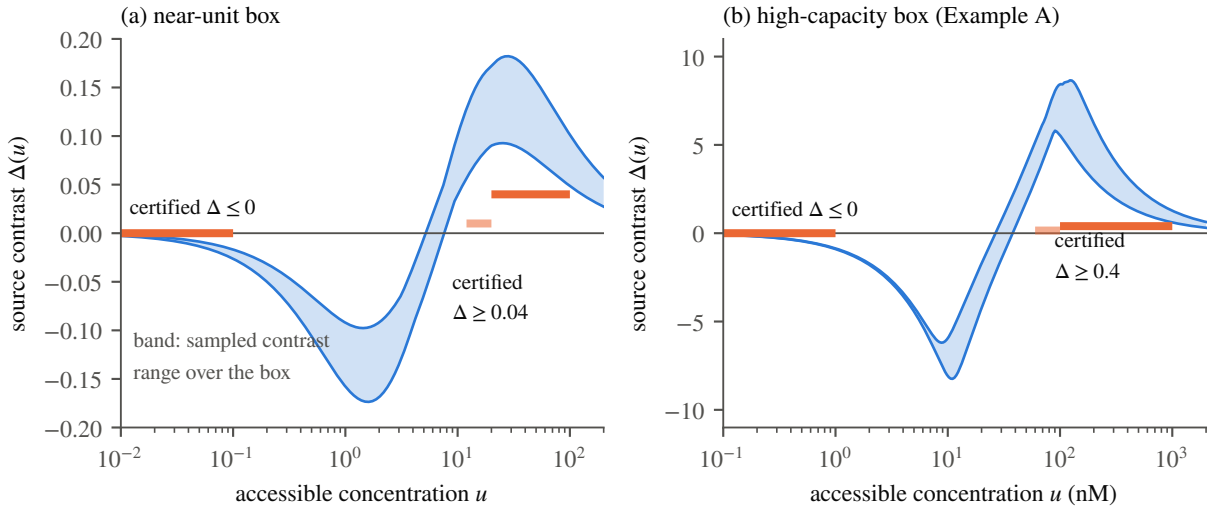

Figure 3: Certified statements (thick segments) against the range of the source contrast sampled over the corners of the calibration box (band). (a) Near-unit box: $\Delta \le 0$ on $[0, 0.4]$ (shown from 0.01), $\Delta \ge 0.04$ on $[20, 100]$, and the alternative $\Delta \ge 0.01$ from 12 (faint). (b) Example 4.4: $\Delta \le 0$ up to 15 nM (shown to 1), $\Delta \ge 0.4$ on $[100, 1000]$ nM and $\Delta \ge 0.15$ from 60 nM (faint). The band is a numerical illustration.

certified only $\frac{3}{2500}$; retaining the shared product CD improved the guarantee by a factor of $100/3$ without changing any assumption. By Theorem 3.1(iv) the sign of Δ flips at the crossover $u^\dagger$, which depends on the unknown parameters: over the corners of the near-unit box it ranges numerically over about $[5.20, 7.58]$, and over $[26.6, 37.8]$ nM for Example 4.4. No sign-based rule can therefore have an accessible low threshold above, or a high threshold below, those intervals; a guard band is intrinsic, not an artefact of the proof.

5 From source margins to decisions

5.1 Error budgets

Proposition 5.1 (Noise wrapper; L for equal allowances)**.** *Suppose a source statement gives $\Delta \le 0$ on a low class and $\Delta \ge m$ on a high class, and $|e_1| \le \varepsilon_1$, $|e_d| \le \varepsilon_d$, $g \ge g_{\min} > 0$. Then $Z \le \varepsilon_1 + \varepsilon_d$ on the low class and $Z \ge g_{\min} m - \varepsilon_1 - \varepsilon_d$ on the high class; the threshold rule is correct whenever $2(\varepsilon_1 + \varepsilon_d) < g_{\min} m$. If instead a direct bound $|e_d - e_1| \le \delta$ is available, $g_{\min} m > 2\delta$ suffices.*

A truly shared additive offset cancels in Z and must not be counted twice; different specimen backgrounds must not be assumed to cancel.

5.2 Reporting without a binary promise

For the concrete contract $g_{\min} = 1$, $\varepsilon = 10^{-4}$ put $a_* = \frac{1}{5000}$ and $b_* = \frac{199}{5000}$.

Corollary 5.2 (One-sided exclusions; L)**.** *Under the near-unit contract, with no assumption on the class of x,*

$$Z > a_* \implies x > \tfrac{1}{10}, \qquad Z < b_* \implies x \notin [25, 100]. \tag{5.1}$$

If a ceiling $x \le 100$ is independently justified, $a_* < Z < b_*$ implies $\frac{1}{10} < x < 25$.

The inequalities are strict contrapositives of (4.2). Neither $Z \le a_*$ nor $Z \ge b_*$ alone establishes the corresponding class. (The compiled statement uses the low threshold $\frac{1}{10}$; by (4.1) the same holds with $\frac{2}{5}$.)

Outer enclosures. Let $\mathcal{C}(y_1, y_d)$ be the set of native concentrations for which some admissible parameters, gains and errors reproduce the readings, and $\mathcal{C}_U = \mathcal{C} \cap [0, U]$ for a declared ceiling U. The true concentration always belongs to $\mathcal{C}$, and to $\mathcal{C}_U$ if $x \le U$ (L). An implementation that computes an outer set $\mathcal{O}_U \supseteq \mathcal{C}_U$ may therefore report, in this order: *incompatible* if $\mathcal{O}_U = \emptyset$; *low* if $\mathcal{O}_U \subseteq [0, 0.1]$; *high* if $\mathcal{O}_U \subseteq [25, U]$; and *unresolved* otherwise. Our exact-rational implementation bisects accessible concentration, in the manner of interval branch-and-prune [20]. For a cell $[l, h]$ it evaluates the necessary conditions obtained from (2.4) on the cell, from $d \in [9, 11]$ and $r \in [\frac{19}{20}, \frac{21}{20}]$, and from the two observation intervals; each reading constrains the *same* gain $g \ge 1$, and the two gain intervals are intersected before a cell is retained. The contrast cuts (5.1) are further necessary tests. A cell is discarded only if a necessary condition fails on all of it, the two halves cover their parent, and a surviving cell $[l, h]$ projects to the native set $[l, \frac{5}{4}h] \cap [0, U]$. By induction on depth every admitted true state survives: finite depth affects tightness, never soundness (C). A retained cell is not asserted to be feasible, and the program is not itself formally verified. It keeps disconnected sets, accepts missing or censored readings as intervals, and abstains when no finite ceiling is supplied rather than replacing infinity by a large number.

5.3 From a precision profile to an error allowance

Assay imprecision is usually reported as a coefficient of variation along the measuring range [6, 29]. A coefficient of variation is a standard-deviation statement, a deterministic bound $|e| \le \varepsilon$ is not, and a normal error has no finite bound that holds with probability one [16]. The bridge has two layers. The decision is correct whenever all calibration and error assumptions hold; a separate measurement model states how often they hold.

Write $e_j = \beta'_j + \xi_j$ with a justified residual-bias bound $|\beta'_j| \le \beta_j$ and, at the relevant state, ξ_j centred normal with standard deviation at most σ_j. With

$$k = \Phi^{-1}(1 - \alpha/4), \qquad \varepsilon_j = \beta_j + k\sigma_j \quad (j = 1, d), \tag{5.2}$$

each of the four tail events has probability at most $\alpha/4$, and the union bound gives simultaneous coverage at least $1 - \alpha$ without any independence assumption. The resulting guarantee is a repeated-experiment coverage for each fixed specimen state. It is not a posterior probability of "low" or "high", and not an error rate conditional on having selected specimens with unusually low first readings. Estimated standard deviations need their own confidence or tolerance construction, and unknown calibration quantities consume their own share of α.

Example 5.3 (Synthetic budget)**.** For the $m = 0.04$ certificate suppose that both true normalised means are at most 0.2, that the random standard deviation is at most 1% of signal (hence at most 0.002, blank noise included) and that each residual bias is at most 0.001. For $\alpha = 0.01$, $k \approx 2.807034$ and $\varepsilon \approx 0.00661407 < 0.01$: the decision is correct on an event of probability at least 99%, with admissible contrast bounds about 0.01323 (low) and 0.02677 (high). If the contrast is calibrated directly, independent errors give the two-sided 99% allowance $\delta = 0.002 + \Phi^{-1}(0.995)\sqrt{2}\,(0.002) \approx 0.00928555 < m/2$; in general $\mathrm{Var}(\xi_d - \xi_1) = \sigma_d^2 + \sigma_1^2 - 2\,\mathrm{Cov}(\xi_d, \xi_1)$ and the covariance term may not be dropped [16].

Near the blank a coefficient of variation is unstable and an absolute component is needed, e.g. $\sigma(s)^2 = \sigma_0^2 + (vs)^2$. Replicates reduce only the independent random component.

5.4 Bounded relative error is gain drift

An unbounded common gain makes a global absolute standard deviation unnatural. Suppose instead

$$Y_1 = gB(u)(1+\xi_1) + a_1, \qquad Y_d = grB(u/d)(1+\xi_d) + a_d, \qquad |\xi_1|, |\xi_d| \le \eta < 1, \quad |a_1|, |a_d| \le \varepsilon_0. \tag{5.3}$$

Proposition 5.4 (Relative-error reduction; L). *With $g' = g(1+\xi_1)$ and $r' = r(1+\xi_d)/(1+\xi_1)$ the readings (5.3) have exactly the form (2.6), with*

$$g' \ge g_{\min}(1-\eta), \qquad r' \in \Big[r_{\min}\frac{1-\eta}{1+\eta},\ r_{\max}\frac{1+\eta}{1-\eta}\Big]. \tag{5.4}$$

For the near-unit box and $\eta = \frac{3}{100}$ this interval is $[\frac{1843}{2060}, \frac{2163}{1940}]$; the low sign persists on $[0, \frac{1}{10}]$ because $\frac{2163}{1940} \cdot \frac{1}{9} = \frac{721}{5820} < \frac{3}{20}$, the source margin on $[20, 100]$ is at least $\frac{3}{100}$, and

$$Z \le 2\varepsilon_0 \quad \textit{(low)}, \qquad Z \ge \tfrac{97}{100} \cdot \tfrac{3}{100}\, g_{\min} - 2\varepsilon_0 \quad \textit{(high)}.$$

Relative imprecision thus consumes the gain-drift budget, and the certificate must be recomputed on the wider interval; the old margin must not be kept. At $g_{\min} = 1$ and $\varepsilon_0 = 0.001$ the bounds are 0.002 and 0.0271. A 3% relative *envelope* is not a 3% coefficient of variation: for centred normal relative errors with standard deviation 1% the envelope holds for both readings with probability at least $1 - 4\Phi(-3) \approx 0.9946$. The same fluctuation must not be counted in both r and ξ.

6 Exact limits on inference

Each obstruction below is an observational equivalence: two admissible worlds produce identical data. They point to different remedies, and only one of them is cured by more precise measurement.

6.1 A neat reading alone

Proposition 6.1 (Neat collision; L). *The states (3.2) satisfy (2.1) for unit parameters, have equal signals, and with $\rho = 1$ lie in the low and high classes of Theorem 4.1. With equal gains and zero error no function of the neat reading classifies both correctly.*

By Theorem 3.1(ii) the same happens for every parameter choice and every pair $u_\pm(s)$ that straddles the declared classes, and no amount of replication of the neat reading helps. The statement concerns nonabstaining rules that must start from this neat reading. It does not rule out a redesigned single reading, and it is fully consistent with upfront-dilution workflows [35]. Calibrators, blanks, specimen volume and incubation time are separate costs.

6.2 Accessible spikes do not identify native availability

Suppose a post-dilution spike s is fully accessible while native masking persists, so that every permitted response is a function of $\rho x/d + s$.

Proposition 6.2 (Masking; L). *The worlds* $(x, \rho) = (\frac{1}{10}, 1)$ *and* $(100, \frac{1}{1000})$ *induce the same response for every dilution* d*, every spike* s *and every response function. Hence no rule on the complete action–response map, and in particular no deterministic adaptive choice of spikes and dilutions, separates them. More generally, if* $0 < \rho_{\min} \le \rho \le \rho_{\max}$ *and* $\rho_{\min} H \le \rho_{\max} L$*, the native states* $(H, \rho_{\min})$ *and* $(\rho_{\min} H/\rho_{\max}, \rho_{\max})$ *have the same accessible concentration, the second lies in the class* $x \le L$*, and an accessible interval* $[u_-, u_+]$ *yields exactly*

$$x \in [u_-/\rho_{\max},\ u_+/\rho_{\min}]. \tag{6.1}$$

Spike recovery can be ideal on the accessible scale in both worlds; the second world lies outside the availability contract of Theorem 4.1, as it must. For $L > 0$, a necessary condition for separating $x \le L$ from $x \ge H$ from accessible-only measurements is $H/L > \rho_{\max}/\rho_{\min}$, and for exactly known u both endpoints of (6.1) are attained. Under $\rho \in [0.8, 1]$ the residual factor is 1.25; once it dominates, a native-recovery measurement is worth more than a more precise repeat of the same accessible signal. This is a statement about the stated action model. A spike that demonstrably behaves like native analyte under a quantified preparation (the premise of parallelism and recovery validation [4, 14]) supplies different information and must be modelled as such.

6.3 A finite panel cannot exclude an unbounded noisy tail

Proposition 6.3 (Blank-compatible tail; L). *For the near-unit reagent box, unit gain,* $\rho = 1$ *and any dilution* $0 < d \le M$*,*

$$0 \le B(x/d) \le \frac{121\, d}{100\, x} \le \frac{121M}{100x}, \tag{6.2}$$

so if $\varepsilon > 0$ *and* $x \ge 121M/(100\varepsilon)$ *the all-zero transcript lies within the error allowance of every reading of the panel, exactly as it does for a blank.*

The same argument applies along the finite all-blank path of a deterministic adaptive procedure. No claim is made for randomised protocols, unbounded dilution ranges or additional measurement channels. For $M = 11$ and $\varepsilon = 10^{-4}$ every $x \ge 133100$ is blank-compatible (Figure 4). Combined with Proposition 4.3: at a fixed bounded dilution range and error model, the ceilings that can be certified and the ceilings that cannot both scale as $1/\varepsilon$. The constants do not match and no minimax claim is made.

6.4 Ideal identifiability and the noisy tail are compatible

By Theorem 3.1(iii), for known parameters and noise-free readings the ratio $Y_d/(rY_1) = R(u)$ identifies u exactly, on the whole half-line. There is no contradiction with Proposition 6.3: along the tail the ratio approaches its limit d while both raw signals vanish, and by (2.5)

$$\Delta(u) = \frac{CD(rd-1)}{u} - \frac{CD(K+J)(rd^2-1)}{u^2} + O(u^{-3}). \tag{6.3}$$

The sign of the contrast stays positive while its size tends to zero. Injectivity at every finite state does not give stable identification uniformly over an unbounded range, and a more powerful fitting algorithm cannot substitute for a justified concentration ceiling.

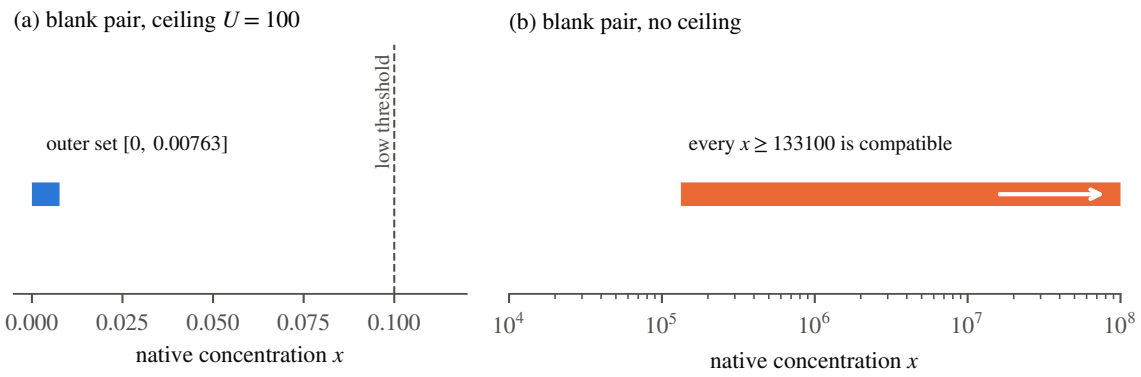

Figure 4: The same pair of blank readings under two domain assumptions ($g_{\min} = 1$, $\varepsilon = 10^{-4}$, dilutions at most 11). (a) With a declared ceiling $U = 100$ the computed outer set is $[0, 125/16384]$, a *low* report. (b) Without a ceiling every $x \geq 133100$ is compatible; the bar shows a subset of the compatible set, which continues to infinity.

7 Departures from the ideal protocol

7.1 Availability that changes on dilution

Let $u = \rho_1 x$ and $\kappa = \rho_d/\rho_1 > 0$. The diluted accessible concentration is $\kappa u/d = u/d_{\text{eff}}$ with $d_{\text{eff}} = d/\kappa$, and for positive interval bounds $d_{\text{eff}} \in [d_-/\kappa_+,\ d_+/\kappa_-]$.

Proposition 7.1 (Availability drift; L). *For the near-unit box with $\kappa \in [\frac{19}{20}, \frac{21}{20}]$ the effective dilution lies in $[\frac{60}{7}, \frac{220}{19}]$, the source margin on $u \in [20, 100]$ is at least $\frac{3}{100}$, and the low sign persists because $\frac{21}{20} \cdot \frac{7}{60} < \frac{3}{20}$.*

The extension consumes margin, because the dilution interval has really widened. Shared C, D, K, J and the observation model remain necessary; altered affinities, nonspecific adsorption and unknown backgrounds are not absorbed by d_{eff}.

7.2 A calibrated attenuation bound suffices

Proposition 7.2 (Transient signals; L). *Suppose the actual source signals satisfy*

$$\tfrac{9}{10} B(u) \leq T_1 \leq B(u), \qquad \tfrac{9}{10} B(u/d) \leq T_d \leq B(u/d). \tag{7.1}$$

For the near-unit box, $rT_d - T_1 \leq 0$ for $u \leq \frac{1}{10}$ and $rT_d - T_1 \geq \frac{3}{100}$ for $u \in [20, 100]$; with noise, the high contrast is at least $\frac{3}{100} g_{\min} - 2\varepsilon$.

For low u the proof uses $[(21/20)/9 - (9/10)(3/20)]u \leq 0$; for high u, $rT_d - T_1 \geq (\frac{9}{10} r) B(u/d) - B(u)$ and the polynomial certificate with $r_0 = \frac{171}{200}$. The multiplicative form matters: g has no upper bound, so a small source discrepancy is not a small additive signal error.

7.3 From rate constants to a sufficient incubation time

Proposition 7.2 leaves open how (7.1) is to be established. Equilibrium calibration alone cannot do it, since scaling all on- and off-rates by a small factor preserves K, J and slows the dynamics arbitrarily. For a well-mixed solution-phase reaction, rate constants do suffice.

Consider mass-action kinetics of the four analyte species A_{ij} ($i,j \in \{0,1\}$ the occupancies of the capture and detector sites), in which capture reagent binds either species with a free capture site at rate k_{on}^{C} and dissociates at rate $k_{\mathrm{off}}^{C} = K k_{\mathrm{on}}^{C}$, the detector likewise with k_{on}^{D} and $k_{\mathrm{off}}^{D} = J k_{\mathrm{on}}^{D}$, independently of the other site. All analyte is unbound at $t = 0$. Let $T(t) = A_{11}(t)$ and

$$\lambda_C(u) = k_{\mathrm{on}}^{C}\sqrt{(u - C)^2 + 2K(u + C) + K^2}, \tag{7.2}$$

with λ_D defined analogously.

Theorem 7.3 (Kinetic bridge; C)**.** *In the setting just described, for every $u > 0$:*

(i) $A_{11} = upq$, $A_{10} = up(1-q)$, $A_{01} = u(1-p)q$, $A_{00} = u(1-p)(1-q)$, *where* $p(0) = q(0) = 0$ *and*

$$\dot{p} = k_{\mathrm{on}}^{C}\{(C - up)(1-p) - Kp\}, \qquad \dot{q} = k_{\mathrm{on}}^{D}\{(D - uq)(1-q) - Jq\}.$$

(ii) p *increases to the equilibrium root* p_* *with* $0 \le p_* - p(t) \le p_* e^{-\lambda_C(u)t}$, *and similarly for* q.

(iii) For all $t \ge 0$,

$$\bigl(1 - e^{-\lambda_C(u)t}\bigr)\bigl(1 - e^{-\lambda_D(u)t}\bigr)\, B(u) \le T(t) \le B(u). \tag{7.3}$$

(iv) $\lambda_C(u) \ge k_{\mathrm{on}}^{C} \max\{K,\, 2\sqrt{CK}\}$ *for every* $u \ge 0$.

Proof. (i) With the product ansatz the free capture reagent is $C - A_{10} - A_{11} = C - up$ and the free detector is $D - uq$. Substituting, for instance,

$$\dot{A}_{11} = k_{\mathrm{on}}^{C}(C - up)A_{01} - k_{\mathrm{off}}^{C}A_{11} + k_{\mathrm{on}}^{D}(D - uq)A_{10} - k_{\mathrm{off}}^{D}A_{11} = u(\dot{p}\,q + p\,\dot{q}),$$

and the other three equations are verified in the same way. The right-hand sides are polynomial, so the solution of the initial-value problem is unique and equals the product form. (ii) Let $f(p) = k_{\mathrm{on}}^{C}\{(C - up)(1-p) - Kp\}$. Then $f(p_*) = 0$, $f > 0$ on $[0, p_*)$, and by uniqueness $p(t) < p_*$ for all t, so p is increasing. On $[0, p_*]$,

$$f'(p) = -k_{\mathrm{on}}^{C}(u + C + K - 2up) \le -k_{\mathrm{on}}^{C}(u + C + K - 2up_*) = -\lambda_C(u),$$

because up_* is the smaller root of $w^2 - (u + C + K)w + uC = 0$, that is $2up_* = u + C + K - \sqrt{(u + C + K)^2 - 4uC}$. By the mean value theorem $y = p_* - p$ satisfies $\dot{y} = -f(p) \le -\lambda_C y$, hence $y \le p_* e^{-\lambda_C t}$. (iii) follows from (i), (ii) and $B = up_*q_*$. (iv) The radicand equals $(u+K-C)^2 + 4CK \ge 4CK$, and also $(u - C)^2 + 2K(u + C) + K^2 \ge (|u - C| + K)^2 \ge K^2$. □

Corollary 7.4 (Sufficient incubation; C)**.** *Let* $\lambda_* = \min\{k_{\mathrm{on}}^{C} \max(K, 2\sqrt{CK}),\, k_{\mathrm{on}}^{D} \max(J, 2\sqrt{DJ})\}$, *minimised over the calibration box. If both reactions are read at a common time* $t \ge 3/\lambda_*$, *then* (7.1) *holds for every* $u \ge 0$ *and every* d, *because* $(1 - e^{-3})^2 \approx 0.9029$ *(the exact requirement is* $\lambda_* t \ge -\log(1 - \sqrt{0.9}) \approx 2.9697$*). Proposition 7.2 then applies.*

For the near-unit box and for Example 4.4 alike, $2\sqrt{CK} \ge 1.8$ nM; with $c_0 = 1$ nM and $k_{\mathrm{on}} = 10^6\,\mathrm{M^{-1}s^{-1}} = 10^{-3}\,\mathrm{nM^{-1}s^{-1}}$ for both sites this gives $\lambda_* \ge 1.8 \times 10^{-3}\,\mathrm{s^{-1}}$ and a sufficient incubation of about 28 minutes (a synthetic illustration). For unit parameters the bound is attained as $u \to 0$; it is conservative at high concentration, where binding is fast (Figure 5). The theorem is about homogeneous mass-action kinetics; diffusion-limited surface binding and lateral flow [21, 22] need their own bridge, and a flat measured time trace does not by itself establish the factorisation in (i).

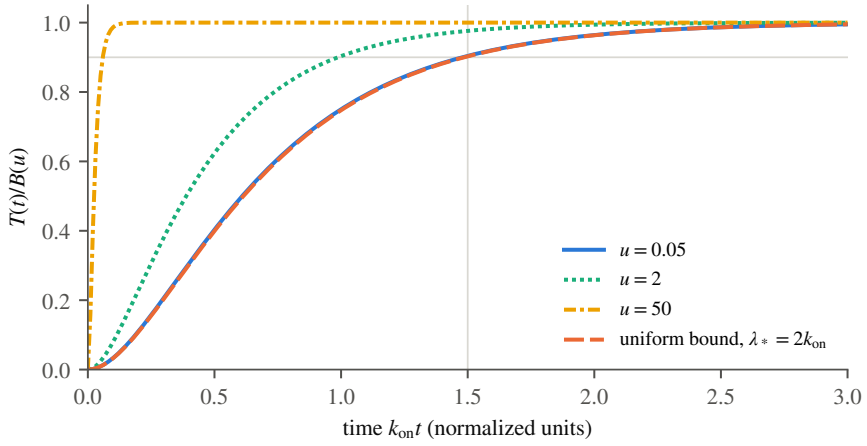

Figure 5: Approach to equilibrium of the sandwich concentration for unit parameters and equal on-rates, against the uniform bound (7.3) with $\lambda_* = 2k_{\mathrm{on}}$. The 90% level is reached by $k_{\mathrm{on}}t = 1.5$ for every concentration. Numerical illustration of Theorem 7.3.

8 Sequential assays: what washing changes

In a sequential (two-step) format the specimen is first incubated with the capture reagent, unbound material is washed away, and detector is added afterwards [9, 34]. Incomplete washing has long been examined as one source of hook-like behaviour in two-site assays [24, 28], and two-step hooks have also been attributed to multiple-epitope interactions that an antigen-excess partition model does not contain [9]. We give an explicit source model and prove what it implies; it does not describe every solid-phase assay.

Ideal capture, complete wash. The captured amount is $w(u) = up(u; C, K)$, the capture balance of (2.1), equivalently $Kw = (C - w)(u - w)$. Assume complete removal of free analyte, perfect retention of captured analyte, a known detection volume and no loss of capture complexes. Fresh detector with capacity D and constant J then binds the captured analyte with occupancy $q(w; D, J)$, and

$$B_{\mathrm{seq}}(u) = w(u)\, q(w(u); D, J). \tag{8.1}$$

Theorem 8.1 (Ideal washing; L)**.** *w is strictly increasing with $w(u) < \min\{C, u\}$ for $u > 0$ and $0 \le w(u_2) - w(u_1) \le u_2 - u_1$ for $u_1 \le u_2$. Consequently B_{seq} is strictly increasing, and with $b_\infty = C\, q(C; D, J)$,*

$$0 < b_\infty - B_{\mathrm{seq}}(u) \le \frac{KC}{u - C} \qquad (u > C). \tag{8.2}$$

Proof. If $u_1 < u_2$ but $w_1 \ge w_2$, then $Kw_1 = (C - w_1)(u_1 - w_1) \le (C - w_2)(u_1 - w_1) < (C - w_2)(u_2 - w_2) = Kw_2$, a contradiction. If $w_2 - w_1 > u_2 - u_1$, the free analyte decreases while w increases, and $Kw_2 = (C - w_2)(u_2 - w_2) < (C - w_1)(u_1 - w_1) = Kw_1$ contradicts $w_2 > w_1$. The same two facts for the detector stage show that $b(w) = wq(w; D, J)$ is strictly increasing and 1-Lipschitz, so $B_{\mathrm{seq}} = b \circ w$ is strictly increasing and $b_\infty - B_{\mathrm{seq}}(u) \le C - w(u) = Kw/(u - w) \le KC/(u - C)$. □

The ideal response saturates instead of returning to zero: complete washing removes the free analyte that would compete with captured analyte for detector. Saturation still destroys quantitative resolution at high u, and native masking is unaffected.

Table 4: Sequential model at $C = D = 10$, $K = J = 0.1$ nM; $b_\infty \approx 9.048751$. The last row is a mathematical tail illustration, not a plausible concentration.

Accessible u (nM)	Ideal wash $B_{\mathrm{seq}}(u)$	Carry-over $\lambda = 10^{-3}$
1	0.978182	0.978182
10	8.487565	8.487335
100	9.043464	9.004325
1000	9.048271	8.558490
10^6	9.048750	0.099001

Carry-over restores the tail. Suppose a fraction $\lambda \geq 0$ of the free analyte is carried into the detection stage, $a(u) = \lambda\{u - w(u)\}$ in the detection-volume convention, and detector binds captured and carried-over accessible analyte alike. Only detector on captured analyte is read:

$$B_\lambda(u) = w(u)\, q(w(u) + a(u); D, J). \tag{8.3}$$

Proposition 8.2 (Carry-over; L)**.** *Let $q_0 = q(w; D, J)$ and $q_a = q(w + a; D, J)$ with $a \geq 0$. Then $q_a \leq q_0$ and*

$$\frac{B_a}{B_0} = \frac{q_a}{q_0} \geq \frac{D}{D + aq_0} \geq \frac{D}{D + a}. \tag{8.4}$$

If $0 < \beta \leq 1$ and $a\beta \leq D(1 - \beta)$ then $B_a \geq \beta B_0$; in particular

$$\lambda_{\max} U \leq D_{\min}(\beta^{-1} - 1) \implies B_\lambda(u) \geq \beta\, B_{\mathrm{seq}}(u) \quad \text{for } u \leq U,\ \lambda \leq \lambda_{\max}. \tag{8.5}$$

On the other hand, for every $\lambda > 0$ and $u > C$,

$$B_\lambda(u) \leq \frac{CD}{\lambda\,(u - C)}. \tag{8.6}$$

Proof. Dividing the detector balance by the occupancy gives $D/q = v + J/(1 - q)$ at analyte level v. Occupancy decreases in v, so $q_a \leq q_0$ and $D/q_a = w + a + J/(1 - q_a) \leq D/q_0 + a$, which is (8.4). For the tail, $(w+a)q_a \leq D$, $w \leq C$ and $a \geq \lambda(u - C)$ give $B_\lambda = wq_a \leq CD/(w+a) \leq CD/(\lambda(u - C))$. □

Thus the limits do not commute: $\lim_{u\to\infty} B_\lambda(u) = 0$ for every fixed $\lambda > 0$, whereas $\lim_{\lambda\to 0} B_\lambda(u) = B_{\mathrm{seq}}(u) \to b_\infty > 0$. A small carry-over reintroduces the high-dose mechanism at sufficiently high concentration, and (8.5) states how small it must be on a declared range. For example $D_{\min} = 10$ nM, $U = 1000$ nM and $\beta = 0.9$ require $\lambda_{\max} \leq \frac{1}{900} \approx 0.111\%$ carry-over. This is a model-based specification that ignores capture loss and matrix changes, and it guarantees signal retention relative to the ideal washed model, not monotonicity of the imperfectly washed response. Table 4 and Figure 6 illustrate it.

9 Use in assay development

The practical object is a small reproducible calculation, not the inspection of Bernstein coefficients at the bench.

1. *State the decision*: native low and high thresholds, the admitted ceiling, and whether intermediate concentrations may remain unresolved.

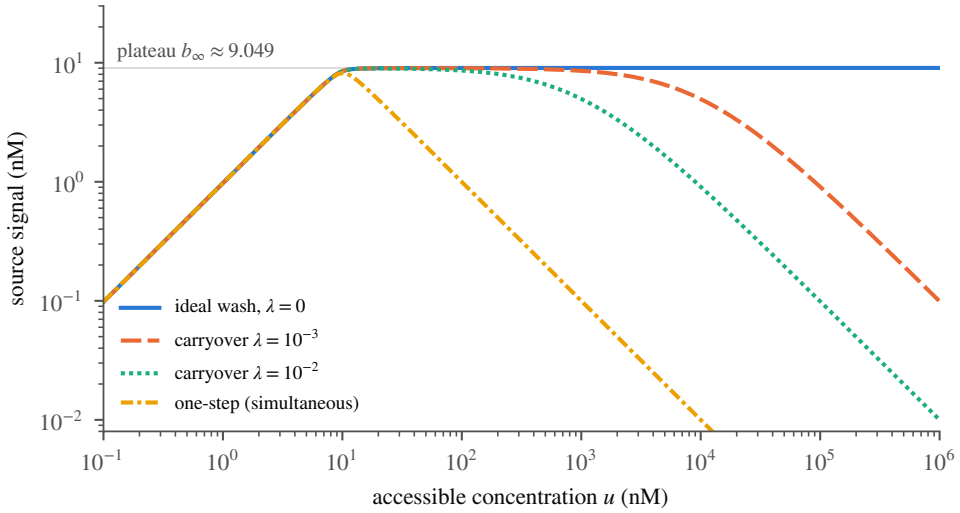

Figure 6: Synthetic source comparison at $C = D = 10$, $K = J = 0.1$ nM. Ideal washing gives a monotone response with plateau b_∞; carry-over fractions 10^{-3} and 10^{-2} restore a $1/u$ tail at high concentration; the one-step response (2.1) hooks as soon as the analyte exceeds the reagent capacity.

2. *Specify the protocol*: simultaneous or sequential binding, order of additions, washing, final volumes, read time, raw measured quantity.
3. *Supply external bounds*: site capacities and affinities, availability, actual dilution, gain drift, linearity, and the error or precision profile; record which are not independently established. Reagent molecule counts need not equal binding-site capacities.
4. *Compute a source margin* with Theorem 4.2 (eight coefficients and (4.8)), or the sequential source of Section 8. If the certificate fails, distinguish a loose bound from a genuine collision using Theorem 3.1 and Remark 4.6.
5. *Compare with the observation budget*: simultaneous absolute allowances, a direct contrast allowance, or the relative-error reduction; allocate probability only where a stochastic model is supported.
6. *Report the admitted inference*: a promised decision, a one-sided exclusion, an outer interval, unresolved, or incompatible, together with the domain and calibration assumptions.
7. *Choose the next informative action*: a matched dilution addresses a neat collision; native-recovery information addresses masking; a justified ceiling or an extended validated panel addresses the tail; a wash study addresses carry-over; an incubation study against Corollary 7.4 addresses equilibration.

Table 5 collects synthetic scenarios. The outer program returns *high* for unit-source $x = 50$ with native enclosure about $[37.415, 100]$, and *incompatible* for a raw reading of -1, which violates the nonnegative-source model by far more than the error allowance; a small negative blank-corrected reading within ε is fully compatible. For the low collision state $x = \frac{200}{2499}$ the outer set is $[0, \frac{1375}{8192}] \approx [0, 0.168]$, which is *unresolved* against the threshold 0.1 although the promised binary rule classifies it correctly: an outer enclosure and a promised decision use different information. A failed

Table 5: Worked synthetic scenarios (near-unit box, $g_{\min} = 1$, $\varepsilon = 10^{-4}$, $U = 100$ unless stated). Retained intervals are outer relaxations.

Observations	Conclusion	Information that matters next
Neat collision (3.2), matched dilution added	Promised low/high states are separated	None for the binary contract
Same neat value, dilution omitted	Two branches remain; unresolved	The matched diluted reading
Native $x = 1$	Guard-band state; unresolved	Refine the target or keep the enclosure
Two blank readings	With $U = 100$: outer set $[0, 0.00763]$, low. Without a ceiling: unresolved	Justify a range or change the panel
Native masking, ideal accessible spike recovery	Identical data for $x = 0.1$ and $x = 100$	Native recovery or changed preparation
$\geq 90\%$ of equilibrium signal, or 5% availability drift	Source margin 0.03	Verify the attenuation (Cor. 7.4) or drift bound

control removes the right to use the calibration assumptions and leads to unresolved reporting, not to a forced label.

For reflex dilution triggered by a low first reading, "the contrast rule is sound once the pair is obtained" must be kept apart from "the trigger captures every relevant high specimen"; the latter needs its own analysis of the first-reading trigger, its errors and the selection it induces. A study aimed at validating the model should retain independently prepared specimen identities, raw neat and diluted signals and backgrounds, actual volumes and timing, run and lot information, censoring, and an independent native concentration or recovery measurement, and should deliberately include cases near the weakest calibration assumptions. Repeated frames of one reaction are not independent specimens. Published dilution studies [13] report concentrations, not the raw paired signals and binding calibration that the certificate needs; none of the numbers in this paper is empirical.

10 Verification, reproducibility and limitations

Formal verification. The L-tagged statements were compiled with Lean 4 (version 4.30.0) and a pinned mathlib [3, 18]. Compilation treats warnings as errors and accepts neither `sorry` nor added axioms; the receipts record source hashes, the toolchain, declaration interfaces and axiom inventories (the standard `propext`, `Classical.choice`, `Quot.sound` only). Table 6 maps statements to declarations in the namespace `SandwichImmunoassay`. The compiled statements quantify over all real parameters in the stated intervals and over all physical roots of (2.1); no separation margin is assumed, and the finite certificates prove the stated real rectangles, not a list of samples. What Lean verifies is the encoded mathematics under its hypotheses. The physical adequacy of (2.1), the calibration of any real assay, the Python reporting program and the correspondence between prose and declarations remain separate responsibilities; the last was checked by hand against the sources. Formal proof has been applied to physical chemistry before [1]; here its role is narrow and practical, namely to remove doubt about inequalities that are uniform over seven real parameters.

Reproducibility. The source package contains the manuscript, the figure and table generators, the exact-rational enclosure program, and a script that replays every number printed in this paper: the Bernstein identities and low-sign conditions in exact arithmetic, and the floating-point illustrations,

Table 6: Statement-to-declaration map (namespace `SandwichImmunoassay`).

Statement	Lean module: declarations
Lemma 2.1	`Source`: `occupancy_exists`, `Occupancy.unique`, `Occupancy.bounds`, `Reaction.envelopes`
Proposition 3.2, (3.2)	`Structure`: `Occupancy.involution`, `signal_involution`; `Source`: `source_endpoint_collision`
Theorem 4.1	`MarginCertificate`: `source_certificate`, `dilution_endpoints`, `noisy_margin`; `OperatingRanges`: `stronger_margin_source`; `GeneralBox`: `near_unit_low_wide`; `Publication`: `publication_main`; `Main`: `specimen_exists`
Theorem 4.2	`GeneralBox`: `general_source_certificate`, `general_dilution_endpoints`, `general_low_sign`
Table 2, Prop. 4.3	`OperatingRanges`: `smaller_guard_source`, `range_1000_source`, `range_10000_source`; `GeneralBox`: `uniform_tail_margin`
Examples 4.4, 4.5	`GeneralBox`: `capacity_high`, `capacity_guard60`, `capacity_low_wide`, `capacity_noisy_high`, `capacity_noisy_low`, `unequal_high`, `unequal_low_wide`
Cor. 5.2, truth containment	`Consequences`: `excludes_low`, `identifies_guard_band`, `truth_within`; `Publication`: `publication_main`
Proposition 5.4	`GeneralBox`: `relative_error_reduction`, `relative_error_high`, `relative_error_low`, `relative_error_noisy_high`, `relative_error_noisy_low`
Props. 6.1–6.3	`Main`: `endpoint_no_classifier`; `Controls`: `no_masking_classifier`, `availability_repair`; `Preparation`: `availability_overlap`; `Obstructions`: `tail_blank`
Props. 7.1, 7.2	`Preparation`: `effective_dilution`, `transient_high`, `transient_low`, `transient_noisy_high`; `OperatingRanges`: `availability_drift_source`
Theorem 8.1, Prop. 8.2	`Sequential`: `Occupancy.captured_strictMono`, `Occupancy.captured_lipschitz`, `sequential_strictMono`, `sequential_below_plateau`, `sequential_plateau_gap`, `carryover_retention`, `wash_specification`, `carryover_tail`
Thms. 3.1, 7.3, Cor. 7.4, enclosure soundness	Conventional proofs in this paper

the involution, the elasticity formula, the monotone ratio, the kinetic bound (against an ODE solver, including the four-species system) and the sequential bounds numerically. The Lean modules and their receipts accompany the repository. Generated curves are synthetic; no clinical dataset is used.

Limitations. The certificates are sufficient, not sharp; the constants in the $1/\varepsilon$ range law do not match the obstruction; and the structure theorem and the kinetic bridge are not yet formalised. The model is homogeneous, noncooperative and two-site. Immobilised-site calibration, multivalency and avidity, cooperative binding [27], transport and residence time in lateral flow [21, 26], heterophilic and matrix interference [31, 33, 32], native commutability and clinical performance all lie outside it. Chemiluminescence is a readout modality and not evidence for a binding protocol, and a lateral-flow control line is not an invariant gain standard [26]. The practical use of the results is to state what an assay must calibrate, what two readings can then exclude, and which missing information cannot be recovered by repeating an indistinguishable control.

A Exact certificate coefficients

Table 7 lists the Bernstein coefficients (4.9) of $Q_m(\cdot, d_\pm)$ in the normalisation (4.7) for every certificate used in the paper. Near-unit rows have $A = H = \frac{11}{5}$, $c = \frac{81}{100}$ (so that $P_m = 100\,Q_m$, the normalisation of Table 1 and of the Lean sources) and $r_0 = \frac{19}{20}$ unless stated; Example 4.4 has $A = H = \frac{1111}{100}$, $c = 81$; Example 4.5 has $A = \frac{1111}{100}$, $H = \frac{1111}{50}$, $c = 162$. All coefficients are positive; the smallest, $447/2500$, occurs for the $[12, 100]$ certificate at $d = 11$, which indicates how little room that alternative has.

Table 7: Bernstein coefficients of all certificates (exact rationals).

certificate	d	b_0	b_1	b_2	b_3
$m = \frac{1}{25}$, $[20, 100]$	9	549739/2500	6249899/2500	23318059/2500	554219/2500
	11	601099/2500	25425377/7500	34047819/2500	26119179/2500
$m = \frac{1}{100}$, $[12, 100]$	9	142047/2500	7251831/2500	9789651/500	108194519/2500
	11	447/2500	26997893/7500	2477943/100	141811479/2500
$m = \frac{1}{200}$, $[20, 10^3]$	9	3321809/2500	163930579/2500	4820411849/2500	2207865619/2500
	11	4019969/2500	620561017/7500	6102058209/2500	5924733579/2500
$m = \frac{1}{2000}$, $[20, 10^4]$	9	1839109/1250	351625757/500	126741925313/625	273117405619/2500
	11	2229769/1250	1325600471/1500	158810410533/625	656586393579/2500
drift, $m = \frac{3}{100}$, $[20, 100]$	60/7	623964/1225	4183164/1225	310236/25	14863164/1225
	220/19	5851116/9025	45832716/9025	177683116/9025	262778316/9025
attenuation, $r_0 = \frac{171}{200}$, $m = \frac{3}{100}$	9	649209/2500	6619929/2500	25577049/2500	19120569/2500
	11	731469/2500	8829389/2500	35892909/2500	43522029/2500
rel. error, $r_0 = \frac{1843}{2060}$, $m = \frac{3}{100}$	9	96648177/257500	791044737/257500	2981865297/257500	2713909857/257500
	11	111738657/257500	1042884017/257500	4121605377/257500	5392702737/257500
Example A, $m = \frac{2}{5}$, $[100, 10^3]$	9	20859839879/10000	243201899759/10000	1576750559639/10000	1105505819519/10000
	11	24898486239/10000	312191285319/10000	2078225484399/10000	2407001083479/10000
Example A, $m = \frac{3}{20}$, $[60, 10^3]$	9	189467991/1000	160028623863/10000	243938250477/1250	4130450819769/10000
	11	59176431/1000	200486296783/10000	308422184157/1250	5555389293729/10000
Example B, $m = \frac{4}{5}$, $[200, 10^3]$	9	41918049839/2500	197023156399/2500	620461062959/2500	288231769519/2500
	11	54016762599/2500	793546058677/7500	2637195429557/7500	873666133479/2500

References

[1] M. P. Bobbin, S. Sharlin, P. Feyzishendi, A. H. Dang, C. M. Wraback and T. R. Josephson. Formalizing chemical physics using the Lean theorem prover. *Digital Discovery* 3 (2024), 264–280. doi:10.1039/D3DD00077J.

[2] A. W. Butch. Dilution protocols for detection of hook effects/prozone phenomenon. *Clinical Chemistry* 46 (2000), 1719–1720. doi:10.1093/clinchem/46.10.1719.

[3] L. de Moura and S. Ullrich. The Lean 4 theorem prover and programming language. In *Automated Deduction – CADE 28*, Lecture Notes in Computer Science 12699, Springer, 2021, pp. 625–635. doi:10.1007/978-3-030-79876-5_37.

[4] B. DeSilva, W. Smith, R. Weiner, M. Kelley, J. Smolec, B. Lee, M. Khan, R. Tacey, H. Hill and A. Celniker. Recommendations for the bioanalytical method validation of ligand-binding assays to support pharmacokinetic assessments of macromolecules. *Pharmaceutical Research* 20 (2003), 1885–1900. doi:10.1023/B:PHAM.0000003390.51761.3d.

[5] E. F. Douglass Jr., C. J. Miller, G. Sparer, H. Shapiro and D. A. Spiegel. A comprehensive mathematical model for three-body binding equilibria. *Journal of the American Chemical Society* 135 (2013), 6092–6099. doi:10.1021/ja311795d.

[6] R. A. Dudley, P. Edwards, R. P. Ekins, D. J. Finney, I. G. McKenzie, G. M. Raab, D. Rodbard and R. P. Rodgers. Guidelines for immunoassay data processing. *Clinical Chemistry* 31 (1985), 1264–1271. doi:10.1093/clinchem/31.8.1264.

[7] R. T. Farouki. The Bernstein polynomial basis: a centennial retrospective. *Computer Aided Geometric Design* 29 (2012), 379–419. doi:10.1016/j.cagd.2012.03.001.

[8] S. A. Fernando and G. S. Wilson. Studies of the 'hook' effect in the one-step sandwich immunoassay. *Journal of Immunological Methods* 151 (1992), 47–66. doi:10.1016/0022-1759(92)90104-2.

[9] S. A. Fernando and G. S. Wilson. Multiple epitope interactions in the two-step sandwich immunoassay. *Journal of Immunological Methods* 151 (1992), 67–86. doi:10.1016/0022-1759(92)90105-3.

[10] J. Garloff. The Bernstein algorithm. *Interval Computations* no. 2 (1993), 154–168.

[11] K. L. Hoffman, G. H. Parsons, L. J. Allerdt, J. M. Brooks and L. E. Miles. Elimination of "hook-effect" in two-site immunoradiometric assays by kinetic rate analysis. *Clinical Chemistry* 30 (1984), 1499–1501. doi:10.1093/clinchem/30.9.1499.

[12] A. N. Hoofnagle and M. H. Wener. The fundamental flaws of immunoassays and potential solutions using tandem mass spectrometry. *Journal of Immunological Methods* 347 (2009), 3–11. doi:10.1016/j.jim.2009.06.003.

[13] J. J. H. Hunsaker, S. L. La'ulu, E. Zupan, D. Patel, V. Pandya and J. W. Rudolf. Detection of a high-dose hook effect and evaluation of dilutions of urine myoglobin specimens using a serum myoglobin assay. *Annals of Laboratory Medicine* 44 (2024), 367–370. doi:10.3343/alm.2023.0427.

[14] International Council for Harmonisation. *ICH Harmonised Guideline M10: Bioanalytical Method Validation and Study Sample Analysis*. Final version, adopted 24 May 2022. `https://database.ich.org/sites/default/files/M10_Guideline_Step4_2022_0524.pdf`.

[15] J. F. M. Jacobs, R. G. van der Molen, X. Bossuyt and J. Damoiseaux. Antigen excess in modern immunoassays: to anticipate on the unexpected. *Autoimmunity Reviews* 14 (2015), 160–167. doi:10.1016/j.autrev.2014.10.018.

[16] Joint Committee for Guides in Metrology. *Evaluation of measurement data — Guide to the expression of uncertainty in measurement*. JCGM 100:2008, BIPM, 2008. doi:10.59161/JCGM100-2008E.

[17] C. F. Manski. *Partial Identification of Probability Distributions*. Springer Series in Statistics, Springer, New York, 2003. doi:10.1007/b97478.

[18] The mathlib Community. The Lean mathematical library. In *Proceedings of the 9th ACM SIGPLAN International Conference on Certified Programs and Proofs (CPP 2020)*, ACM, 2020, pp. 367–381. doi:10.1145/3372885.3373824.

[19] L. E. M. Miles and C. N. Hales. Labelled antibodies and immunological assay systems. *Nature* 219 (1968), 186–189. doi:10.1038/219186a0.

[20] R. E. Moore, R. B. Kearfott and M. J. Cloud. *Introduction to Interval Analysis*. SIAM, Philadelphia, 2009. doi:10.1137/1.9780898717716.

[21] S. Qian and H. H. Bau. A mathematical model of lateral flow bioreactions applied to sandwich assays. *Analytical Biochemistry* 322 (2003), 89–98. doi:10.1016/j.ab.2003.07.011.

[22] E. G. Rey, D. O'Dell, S. Mehta and D. Erickson. Mitigating the hook effect in lateral flow sandwich immunoassays using real-time reaction kinetics. *Analytical Chemistry* 89 (2017), 5095–5100. doi:10.1021/acs.analchem.7b00638.

[23] D. Rodbard and Y. Feldman. Kinetics of two-site immunoradiometric ('sandwich') assays—I. Mathematical models for simulation, optimization, and curve fitting. *Immunochemistry* 15 (1978), 71–76. doi:10.1016/0161-5890(78)90045-7.

[24] D. Rodbard, Y. Feldman, M. L. Jaffe and L. E. M. Miles. Kinetics of two-site immunoradiometric ('sandwich') assays—II. Studies on the nature of the 'high-dose hook effect'. *Immunochemistry* 15 (1978), 77–82. doi:10.1016/0161-5890(78)90046-9.

[25] D. Rodbard and G. H. Weiss. Mathematical theory of immunoradiometric (labeled antibody) assays. *Analytical Biochemistry* 52 (1973), 10–44. doi:10.1016/0003-2697(73)90328-X.

[26] G. M. S. Ross, D. Filippini, M. W. F. Nielen and G. IJ. Salentijn. Unraveling the hook effect: a comprehensive study of high antigen concentration effects in sandwich lateral flow immunoassays. *Analytical Chemistry* 92 (2020), 15587–15595. doi:10.1021/acs.analchem.0c03740.

[27] R. D. Roy, C. Rosenmund and M. I. Stefan. Cooperative binding mitigates the high-dose hook effect. *BMC Systems Biology* 11 (2017), 74. doi:10.1186/s12918-017-0447-8.

[28] R. G. Ryall, C. J. Story and D. R. Turner. Reappraisal of the causes of the "hook effect" in two-site immunoradiometric assays. *Analytical Biochemistry* 127 (1982), 308–315. doi:10.1016/0003-2697(82)90178-6.

[29] W. A. Sadler, M. H. Smith and H. M. Legge. A method for direct estimation of imprecision profiles, with reference to immunoassay data. *Clinical Chemistry* 34 (1988), 1058–1061. doi:10.1093/clinchem/34.6.1058.

[30] N. Sathishkumar and B. J. Toley. Development of an experimental method to overcome the hook effect in sandwich-type lateral flow immunoassays guided by computational modelling. *Sensors and Actuators B: Chemical* 324 (2020), 128756. doi:10.1016/j.snb.2020.128756.

[31] C. Selby. Interference in immunoassay. *Annals of Clinical Biochemistry* 36 (1999), 704–721. doi:10.1177/000456329903600603.

[32] C. M. Sturgeon and A. Viljoen. Analytical error and interference in immunoassay: minimizing risk. *Annals of Clinical Biochemistry* 48 (2011), 418–432. doi:10.1258/acb.2011.011073.

[33] J. Tate and G. Ward. Interferences in immunoassay. *The Clinical Biochemist Reviews* 25 (2004), 105–120.

[34] D. Wild (ed.). *The Immunoassay Handbook: Theory and Applications of Ligand Binding, ELISA and Related Techniques*, 4th ed. Elsevier, Oxford, 2013.

[35] S. J. Wu and J. A. Hayden. Upfront dilution of ferritin samples to reduce hook effect, improve turnaround time and reduce costs. *Biochemia Medica* 28 (2018), 010903. doi:10.11613/BM.2018.010903.